BLIND SOURCE SEPARATION FOR SURFACE ELECTROMYOGRAMS USING A BAYESIAN APPROACH

Mahtab Aboufazeli and V John Mathews

School of Electrical Engineering and Computer Science
Oregon State University
Corvallis, OR 97331, USA

ABSTRACT

This paper presents a blind source separation algorithm to identify binary and sparse sources from convolutive mixtures with linear and time-invariant finite impulse responses. Our approach combines Bayesian algorithms for detecting source activity with a linear minimum mean-square error estimator to identify all the time samples when each source is active. The algorithm was implemented on simulated electromyograms to identify neural commands. Our algorithm identified more than 96% of the sources on average with 16 or more measurement channels and SNR $\geq$ 14 dB. For the detected sources, this algorithm correctly identified more than 94% of the samples on average. This performance was significantly better than that of a competing algorithm available in the literature.

Index Terms— Blind source separation, Bayesian classification, Linear minimum mean-square error estimator, Sparsity-aware processing

I. INTRODUCTION

Electromyograms (EMGs) quantify the electrical activity of a muscle or a group of muscles. EMG signals can be recorded using surface electrodes placed on the skin (sEMG) or from the muscles directly using intramuscular electrodes (iEMG), and are employed in various applications including movement intent decoding to control prostheses [1], [2], stroke rehabilitation systems [3], and other human machine interface systems [4].

Although neural excitation during planning and execution of movements result in the generation of electromyograms, the recorded EMG signals obtained using multiple electrodes are diffused and mixed versions of the neural source signals because these bioelectric signals arrive at the sensors after traveling through nerves and tissues in the body. This paper presents a blind source separation (BSS) algorithm that identifies the neural activities that resulted in the recorded EMG signals. Accurate source separation will lead to better algorithms for predicting movement intent using EMG signals. The algorithm is derived assuming that the recorded signals are convolutive mixtures of the neural source signals, and that the neural source signals are sparse and binary.

A number of BSS methods have been employed to identify the source signals in electromyograms for different applications. Farina *et al.* [5] used an approach based on spatial time-frequency distributions to separate sEMG signals using a linear instantaneous mixture model. Holobar and Zazula [6], [7] modeled EMG measurements as convolutive mixtures of sparse and binary sources with time invariant and finite length impulse responses and presented two BSS algorithms that did not require any prior information of the sources. In a later study, Holobar [8] showed that the EMG decomposition algorithm presented in [7] can theoretically separate synchronized sources in tremor affected patients. Stachaczyk *et al.* [9] employed the BSS technique of [6] to track transient phases of muscle activation during voluntary contractions. Negro *et al.* [10] combined convolutive sphering [11] and fast-ICA [12] to derive a BSS algorithm based on a convolutive mixture model. Monsifrot *et al.* [13] introduced a BSS algorithm based on Markov Decision Process models and Bayesian filtering. Zhu *et al.* [14] developed a BSS algorithm for high density sEMG signals by employing a contrast function maximization approach.

Most of the algorithms in the literature require a high number of measurement channels, high SNR values and short impulse responses. Performance evaluation has indicated that the algorithm of this paper could identify sources with small number of measurements and longer impulse responses with relatively low detection error. Although our approach builds upon the BSS algorithm presented by Holobar and Zazula [6], our approach performs significantly better because we employ provably more powerful algorithms to detect activity of the sources. Furthermore, our approach is computationally more efficient that the method in [6].

II. A CONVOLUTIVE MIXTURE MODEL

The sources of the EMG signals are neural commands that are modeled as sparse binary sequences that can take the values 1 or 0, and the probability p that the value is 1 is very small. The neural commands innervate muscle fibers and pass through volume conductors (fat, skin, etc.), and maybe recorded from the surface of the skin as sEMG signals. The combination of muscle responses and volume conductors is

often modeled as a linear and time-invariant system with finite impulse response. That is, we can model the recorded EMG signals as convolutive mixtures of the sources given by [6]

$$x_i(n) = \sum_{j=1}^{N} \sum_{l=0}^{L-1} h_{ij}(l) u_j(n-l) + \zeta_i(n) \quad i = 1, \ldots, M \qquad (1)$$

where $x_i(n)$, $u_j(n)$, and $\zeta_i(n)$ represent the sEMG measured from the i-th measurement channel, the j-th source signal (neural command), and the additive noise in the i-th channel, respectively at time n, and are assumed stationary. In (1), $h_{ij}(l)$ denotes the l-th coefficient of the impulse response corresponding to the i-th measurement channel and the j-th source signal, M, N and L correspond to the number of sEMG channels, the number of neural sources, and the maximum number of coefficients of the impulse responses in the model, respectively.

During times of low or moderate activation, successive spikes of a source signal may be modeled as uncorrelated [15]. However, physiological analyses have suggested that there exists synchronization of distinct pulse trains generated by different sources involved in a specific task [16]. Consequently, the sources are weakly correlated at each time instant. The additive noise sequence in (1) are assumed to be independent of the sources and the coefficients of the impulse response, and are modeled as i.i.d Gaussian processes with zero mean and variance σ_ξ^2.

Let $\underline{X}(n) = [x_1(n), \ldots, x_M(n)]^T$, $\underline{S}(n) = [u_1(n), \ldots, u_1(n-L+1), \ldots u_N(n-L+1)]^T$, and $\underline{Z}(n) = [\zeta_1(n), \ldots, \zeta_M(n)]^T$. Further, let $\underline{H}_i = [h_{i1}(0), \ldots, h_{i1}(L-1), \ldots h_{iN}(L-1)]^T$, and define a coefficient matrix $\mathbf{H} = [\underline{H}_1, \underline{H}_2, \cdots, \underline{H}_M]^T$. Then, (1) can be written compactly as

$$\underline{X}(n) = \mathbf{H}\underline{S}(n) + \underline{Z}(n) = \tilde{\underline{X}}(n) + \underline{Z}(n) \qquad (2)$$

where $\underline{X}(n)$, $\underline{S}(n)$ and $\underline{Z}(n)$ are the vectors of measured EMG signals, source signals that appear in (1), and additive noise samples at time n, respectively, and $\tilde{\underline{X}}(n)$ is the vector of noise-free EMG signals. For later use, let us also define the k-th source vector $\mathbf{S}_k = [s_k(1), s_k(2), \cdots, s_k(Q)]$, where Q represents the number of samples that are analyzed in each channel at any time and $s_k(.)$ represents the k-th element of $\underline{S}(.)$. Note that $s_k(n) \neq u_k(n)$ since $\underline{S}_k(n)$ contains all the source signals at time $n, n-1, \ldots, n-L+1$. Similarly, let us also define an $M \times Q$-element data matrix $\underline{\mathbf{X}}$ whose (k,q)-th element is $x_k(q)$.

III. BAYESIAN BLIND SOURCE SEPARATION

Because of page length restrictions, we provide only a brief description of the derivations here. Figure 1 displays a high-level flow chart of the blind source separation algorithm. As shown in this figure, the algorithm first identifies all values of time n for which at least one entry of $\underline{S}(n)$ is one *i. e.*, at least one source is active at time n. Let V_1 denote the set of all such values of n. The system then picks one of the entries of V_1 (say n_0) and identifies all pairs of time samples of the form (n_0, n) such that at least one source is active at both times n_0 and n. Let $V_2(n_0)$ represent set of values of n so identified. The system then picks an $n_1 \in V_2(n_0)$, determines the set $V_2(n_1)$ similar to $V_2(n_0)$, selects a time instant $n_2 \in V_2(n_0) \cap V_2(n_1)$, determines the set $V_2(n_2)$, and finally $\forall m \in V_3 = V_2(n_0) \cap V_2(n_1) \cap V_2(n_2)$ determines the set $V_2(m)$. We can then show, following the derivations in [6], that for any $m \in V_3$, if the number of elements in $V_4(m) = V_3 \cap V_2(m)$ is sufficiently large (assume this condition is true for $r+1$ number of time samples *e.g.*, $m_0, \ldots, m_r$), with high probability the same source is active at all time samples of $\{n_0, n_1, n_2, m_0, \ldots, m_r\}$. This result allows us to identify the times at which a single source is active. The derivation makes use of the sparsity of the source signals, and assumes that the probability of more than three common spikes in two sources is negligibly small. Once the spike times are identified, a linear minimum mean-square error (LMMSE) estimator is used to estimate the source signals. The process is iterated till all the sources are identified. More details of the single-time and pair-wise activity detection and LMMSE estimation are provided in the rest of this section. A pseudocode for the the complete BSS algorithm is given in Algorithm 1.

III-A. Activity Detection for Each Time Sample

Let $c_0^{(1)}$ denote the hypothesis that no source is active at time n_0 . Under this hypothesis, $\underline{S}(n_0) = \underline{0}$, where $\underline{0}$ is a vector of all zeros or equivalently, $\bigcap_{j=1}^{N_e} \{s_j(n_0) = 0\}$. Similarly, let $c_1^{(1)}$ denote the hypothesis that at least one source is active at time n_0. Under this hypothesis, $\underline{S}(n_0) \neq \underline{0}$. We design a Bayesian classifier for determining the correct hypothesis at each time. For this, we start with

$$P\{\underline{S}(n_0) \in c_q^{(1)} | \underline{X}(n_0)\} = \frac{P\{\underline{X}(n_0) | c_q^{(1)}\} P(c_q^{(1)})}{P\{\underline{X}(n_0)\}} \qquad (3)$$

where $q = 0$ or 1 and $P(c_0^{(1)})$ and $P(c_1^{(1)})$ are *a priori* probabilities of the two classes $c_0^{(1)}$ and $c_1^{(1)}$, respectively. Without loss of generality, we assume a binomial distribution for each source j with the parameter P_s *i.e.*, $P\{s_j(n) = 1\} = P_s$ and a weak correlation between sources j and $k \neq j$ with conditional probability of $P_c = P\{s_j(n) = 1 | s_k(n) = 1\}$. We can show that $P(c_0^{(1)})$ is approximately given by

$$\begin{aligned} P(c_0^{(1)}) &\approx \prod_{j=1}^{N_e - 1} P(s_j(n) = 0 | s_{N_e}(n) = 0) P(s_{N_e}(n) = 0) \\ &\approx \frac{(1 - 2P_s + P_c P_s)^{N_e - 1}}{(1 - P_s)^{N_e - 2}} \end{aligned} \qquad (4)$$

where N_e is the number of elements in the vector $\underline{S}(n)$ and equals $N \times L$. Since $c_0^{(1)}$ and $c_1^{(1)}$ are complementary classes

$$P(c_1^{(1)}) = 1 - P(c_0^{(1)}) \approx 1 - \frac{(1 - 2P_s + P_c P_s)^{N_e - 1}}{(1 - P_s)^{N_e - 2}} \qquad (5)$$

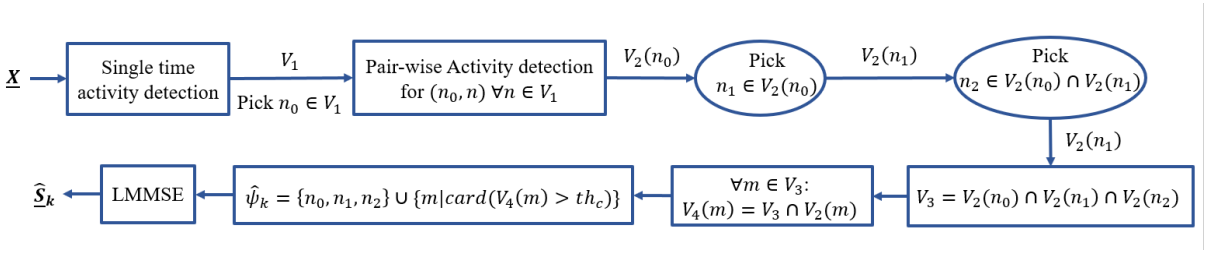

Fig. 1. Flowchart of the BSS algorithm. Details of each block is provided in Section III.

Under our assumptions, we can show that the distribution of $\underline{X}(n)$ conditioned on $\underline{X}(n) \in c_0^{(1)}$ is approximately $N(0, \sigma_\zeta^2 \underline{\mathbf{I}})$ and that the distribution of $\underline{X}(n)$ conditioned on $c_1^{(1)}$ being true is approximately $N(0, \sigma_\zeta^2 \underline{\mathbf{I}} + C_{\underline{\tilde{X}}\underline{\tilde{X}}} \frac{1}{P(c_1^{(1)})})$ where $C_{\underline{\tilde{X}}\underline{\tilde{X}}}$ is the covariance matrix of noise-free EMG signals. In this work, we estimated the noise variance σ_ζ^2 by averaging over the smallest half of the eigenvalues of covariance matrix of measured EMG signals [17] and approximated $C_{\underline{\tilde{X}}\underline{\tilde{X}}}$ using principal component analysis.

Using Bayes theorem, we can compute the log-likelihood ratio of the posterior probabilities and obtain the following classification rule:

$$\frac{1}{2}\underline{X}^T(n_0)\{[C_{\underline{X}\underline{X}}^{(0)}]^{-1} - [C_{\underline{X}\underline{X}}^{(1)}]^{-1}\}\underline{X}(n_0) \underset{c_0^{(1)}}{\overset{c_1^{(1)}}{\gtrless}} \frac{1}{2}\log\left(\frac{|C_{\underline{X}\underline{X}}^{(1)}|}{|C_{\underline{X}\underline{X}}^{(0)}|}\right) + \log\left(\frac{Pr(c_0^{(1)})}{Pr(c_1^{(1)})}\right) \quad (6)$$

where $C_{\underline{X}\underline{X}}^{(0)} = \sigma_\zeta^2 \underline{\mathbf{I}}$ and $C_{\underline{X}\underline{X}}^{(1)} = \sigma_\zeta^2 \underline{\mathbf{I}} + C_{\underline{\tilde{X}}\underline{\tilde{X}}} \frac{1}{Pr(c_1^{(1)})}$.

III-B. Activity Detection at a Pair of Time Samples

Let us use $c_0^{(2)}$ to denote the hypothesis that no source is active at both times n_0 and n_1 or equivalently, $\sum_{j=1}^{N_e} s_j(n_0)s_j(n_1) = 0$, and $c_1^{(2)}$ to denote the hypothesis that at least one source is active at both times n_0 and n_1, or equivalently, $\sum_{j=1}^{N_e} s_j(n_0)s_j(n_1) > 0$, and design a Bayesian classifier for determining the correct hypothesis for each pair of time samples. Using an approach similar to that in Section III-A but lengthier, we can show that the log-likelihood classifier has the form

$$\underline{X}_2^T(n_0, n_1) C_{r_2 r_2} \underline{X}_2(n_0, n_1) \underset{c_0^{(2)}}{\overset{c_1^{(2)}}{\gtrless}} th_2 \quad (7)$$

where $\underline{X}_2(n_0, n_1) = [\underline{X}^T(n_0), \underline{X}^T(n_1)]^T$, $C_{r_2 r_2} = [C_{\underline{X}_2\underline{X}_2}^{(0)}]^{-1} - [C_{\underline{X}_2\underline{X}_2}^{(1)}]^{-1}$, $th_2 = \log(\frac{|C_{\underline{X}_2\underline{X}_2}^{(1)}|}{|C_{\underline{X}_2\underline{X}_2}^{(0)}|}) + 2\log(\frac{Pr(c_0^{(2)})}{Pr(c_1^{(2)})})$,

$$C_{\underline{X}_2\underline{X}_2}^{(0)} \approx \begin{bmatrix} \frac{(P(c_1^{(1)}) - N_e P_c P)}{(P(c_1^{(1)}))^2 - P(c_1^{(2)})} C_{\underline{\tilde{X}}\underline{\tilde{X}}} & \underline{\mathbf{0}} \\ \underline{\mathbf{0}} & \frac{(P(c_1^{(1)}) - N_e P_c P)}{(P(c_1^{(1)}))^2 - P(c_1^{(2)})} C_{\underline{\tilde{X}}\underline{\tilde{X}}} \end{bmatrix} + \sigma_\eta^2 \underline{\mathbf{I}} \quad (8)$$

and

$$C_{\underline{X}_2\underline{X}_2}^{(1)} \approx \begin{bmatrix} \frac{P(1+N_e P_c)}{P(c_1^{(2)})} C_{\underline{\tilde{X}}\underline{\tilde{X}}} & \frac{P}{P(c_1^{(2)})} C_{\underline{\tilde{X}}\underline{\tilde{X}}} \\ \frac{P}{P(c_1^{(2)})} C_{\underline{\tilde{X}}\underline{\tilde{X}}} & \frac{P(1+N_e P_c)}{P(c_1^{(2)})} C_{\underline{\tilde{X}}\underline{\tilde{X}}} \end{bmatrix} + \sigma_\eta^2 \underline{\mathbf{I}} \quad (9)$$

Here, $Pr(c_1^{(2)}) \approx N_e P^2 - \frac{N_e^2}{2} P^2 P_c^2$ and $P(c_0^{(2)}) \approx 1 - N_e P^2 + \frac{N_e^2}{2} P^2 P_c^2$ are *a priori* distributions of class $c_0^{(2)}$ and $c_1^{(2)}$. Detailed derivations are omitted due to space limitations.

III-C. LMMSE Estimator

The LMMSE estimate of the kth source signal $\mathbf{S}_k$ is given by $\hat{\mathbf{S}}_k = C_{\underline{\mathbf{X}}\underline{\mathbf{S}}_k}^T C_{\underline{\mathbf{X}}\underline{\mathbf{X}}}^{-1} \underline{\mathbf{X}}$ where $(\cdot)^T$ denotes the transpose operation, $C_{\underline{\mathbf{X}}\underline{\mathbf{X}}}$ is the covariance matrix of $\underline{X}(n)$ and $C_{\underline{\mathbf{X}}\underline{\mathbf{S}}_k}$ is the cross covariance vector of $\underline{X}(n)$ and $s_k(n)$. Let us denote the set of time samples when the kth source is active as ψ_k, *i. e.*,

$$\psi_k = \{n_{k,1}, n_{k,2}, \ldots n_{k,m_k}\} \quad (10)$$

Given an estimate $\hat{\psi}_k$ of this set $C_{\underline{\mathbf{X}}\underline{\mathbf{S}}_k}$ may be estimated as

$$\hat{C}_{\underline{\mathbf{X}}\underline{\mathbf{S}}_k} = \frac{1}{Q-1} \sum_{n \in \hat{\psi}_k} \underline{X}(n) \quad (11)$$

$C_{\underline{\mathbf{X}}\underline{\mathbf{X}}}$ may be estimated as a time average over the whole interval under analysis.

IV. PERFORMANCE EVALUATIONS

The BSS algorithm was implemented and evaluated on simulated sEMG signals in MATLAB-R2020b.

IV-A. Simulation Environment

The motor unit action potentials (MUAPs), defined by the impulse response signals in the convolutive mixture model of EMG, are the responses of muscles to the neural commands that are recorded by electrodes. In ideal situations where the electrodes are perfectly aligned with muscle fibers, the MUAPs can be modeled by the first-derivative of a Gaussian function [18]. To incorporate some non-idealities into the simulation, we modelled the MUAPs with a summation of the derivative of a Gaussian function and an i.i.d Gaussian noise sequence.

The source signals were modelled as sparse and binary sequences with a binomial distribution with probability $P_s(j) = FR(j)/f_s$ where $FR(j)$ and f_s represent the firing

Algorithm 1 A pseudocode for the BSS algorithm.

Define P_s, P_c, N_e and th_c:
Classify $\underline{S}(n)$ at all time samples using (6)
$V_1 = \{n|\underline{S}(n) \in c_1^{(1)}\}$
Pick $n_0 \in V_1$
Determine set $V_2(n_0) = \{n_1|\underline{S}_2(n_0,n_1) \in c_1^{(2)}\}$
Pick n_1 and n_2 from $V_2(n_0)$ condition on $\underline{S}_2(n_1,n_2) \in c_1^{(2)}$
Determine $V_2(n_1)$ and $V_2(n_2)$ similar to $V_2(n_0)$
$V_3 = V_2(n_0) \cap V_2(n_1) \cap V_2(n_2)$
$\psi_k = \{n_0, n_1, n_2\}$
for all $m \in V_3$ **do**
  $V_4 = V_3 \cap V_2(m)$
  if card$(V_4) > th_c$ **then**
    $\psi_k = \psi_k \cup \{m\}$
  end if
end for
Reconstruct a source using LMMSE estimator
Go to 6 for all pairs of $V_2(n_0)$
$V_1 = V_1 - \{n_0\}$
if card$(V_1) > 1$ **then**
  go to 3
end if

rate of the j-th source signal and the sampling frequency, respectively. Note that the firing rates for different sources are in general different from each other. The inter-spike-intervals (ISI) should be greater than the refractory period since muscle fibers cannot respond to a new spike in this period. The refractory period was defined as the polarization phase of the MUAP (beginning of the MUAP up until its maximum).

Simulated EMG signals were generated with $N = 5$, $f_s = 2000$ Hz, different SNRs from 0dB to 26 dB and four different number of EMG channels *i.e.*, 8, 16, 32, and 64. The firing rate for each source was sampled from a uniform distribution in the range (15 ± 3) and L is sampled from a uniformly distributed random variable in the range (19.76 ± 5.5) samples and then quantized to the smallest integer larger than or equal to the sampled value. The hyper-parameters of the algorithm, *i.e.* $\hat{P}_s$,$\hat{P}_c$ and $\hat{N}_e$ were chosen based on statistics of measurements reported in the literature, and were different from their true values. The performance metrics were the number of detected sources, the source signal detection error and the number of falsely detected sources. The identified sources with more than 30% differences between actual and estimated source signals were considered as falsely detected. If N_d sources were identified, the detection error was defined as

$$e = \frac{1}{N_d} \sum_{k=1}^{N_d} \sum_{n=1}^{D_R} |\hat{u}_k(n) - u_k(n)| \qquad (12)$$

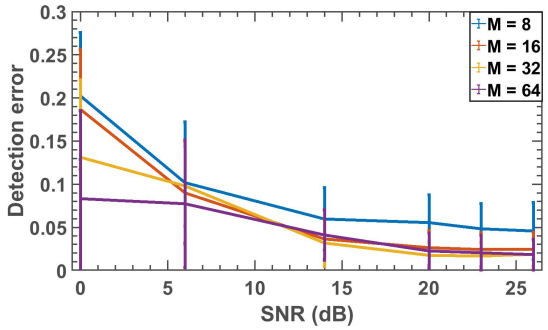

Fig. 2. Detection error as a function of SNR for different number of measurement channels.

IV-B. Results

For each simulation setup, 100 independent runs were performed and the average and standard deviation of detection errors are displayed in Fig. 2 for different number of channels and SNR values. The detection error decreased with increasing number of channels and SNR values. For $SNR \geq 14$ dB, the average error was less than 6%, *i. e.*, the algorithm correctly identified more than 94% of the signal samples generated by the identified sources. The average of the detection error was less than 10% for all simulation setups with $SNR \geq 6$ dB. However, the error was high for $SNR = 0$ dB. In all simulation setups with $M = 8$ and $SNR \geq 20$ dB and for $M \geq 16$ and $SNR \geq 14$ dB, on average at least 4.5 sources out of 5 (90% of total sources) were detected. For $SNR = 6$ dB, on average 2 sources were detected for $M = 8$ and at least 3 sources were detected for $M \geq 16$. The number of falsely detected sources were reduced considerably by increasing the number of measurement channels and SNR in the signal generation model. For $M \geq 16$ and $SNR \geq 20$, and for all other SNR values for $M \geq 32$ on average less than 1 false source was detected. However, this number increased to as much as 3 for the worst cases *i.e.*, $M = 8$ and $SNR = 0$ dB.

We compared our algorithm with the BSS algorithm presented by Holobar and Zazula [6] by separating the sources of the same data sets. In Fig. 3, the number of detected sources as a function of SNR are displayed for $M = 32$. It is clear that our algorithm outperformed the algorithm of [6] by accurately detecting more sources. The detection error metric for the algorithm of [6] was comparable to those of our algorithm. However, it is important to note that this metric is calculated only for the detected sources. As is shown in Figure 3, the algorithm of [6] detects far fewer sources than the algorithm of this paper.

V. CONCLUDING REMARKS

This paper presented a new blind source separation algorithm that decomposes sparse and binary sources of convolutive mixtures. The decomposition algorithm is based

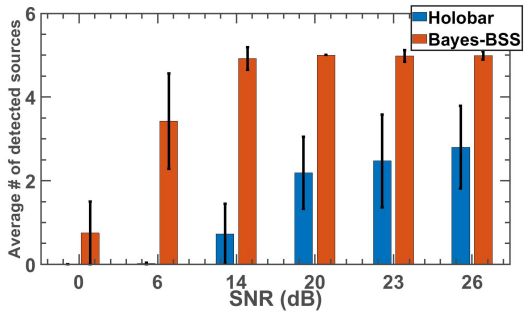

Fig. 3. Comparison of our algorithm and the algorithm of [6] for $M = 32$ as a function of SNR.

on combining an LMMSE estimator with Bayesian activity detectors. Simulations involving realistic EMG models indicated that the method of this paper accurately detects the EMG source signals low level of false detection of sources. In addition, the approach of this paper was able to predict source signals with relatively low errors. Comparison with the algorithm in [6] indicated that our algorithm correctly detected more sources under the same simulation setups. When compared with the methods of [6], our algorithm does not need to generate augmented source channels. Consequently our approach is also computationally more efficient. We are currently exploring using this algorithm in neuroprosthesis systems. Accurate separation of neuronal command signals from their mixtures in EMG measurements should enable more accurate estimation of movement intent from EMG signals than currently possible. This, in turn, should enable prosthesis systems to perform more naturally, with greater accuracy and reduced cognitive load, helping people with limb loss improve the quality of their lives.

ACKNOWLEDGMENT

This work was supported by National Science Foundation Grants 1901492 and 1901236.

VI. REFERENCES

[1] J. E. Ting, A. Del Vecchio, D. Sarma, S. C. Colachis, N. V. Annetta, J. L. Collinger, D. Farina, and D. J. Weber, "Sensing and decoding the neural drive to paralyzed muscles during attempted movements of a person with tetraplegia using a sleeve array," *Journal of Neurophysiology*, vol. 126, no. 6, pp. 2104–2118, Dec 2021.

[2] H. Dantas, D. J. Warren, S. M. Wendelken, T. S. Davis, G. A. Clark, and V. J. Mathews, "Deep learning movement intent decoders trained with dataset aggregation for prosthetic limb control," *IEEE Transactions on Biomedical Engineering*, vol. 66, no. 11, pp. 3192–3203, 2019.

[3] O. W. Samuel, M. G. Asogbon, Y. Geng, N. Jiang, D. Mzurikwao, Y. Zheng, K. K. Wong, L. Vollero, and G. Li, "Decoding movement intent patterns based on spatiotemporal and adaptive filtering method towards active motor training in stroke rehabilitation systems," *Neural Computing and Applications*, vol. 33, no. 10, pp. 4793–4806, 2021.

[4] M. Simão, N. Mendes, O. Gibaru, and P. Neto, "A review on electromyography decoding and pattern recognition for human-machine interaction," *IEEE Access*, vol. 7, pp. 39 564–39 582, 2019.

[5] D. Farina, C. Févotte, C. Doncarli, and R. Merletti, "Blind separation of linear instantaneous mixtures of nonstationary surface myoelectric signals," *IEEE Transactions on Biomedical Engineering*, vol. 51, no. 9, pp. 1555–1567, 2004.

[6] A. Holobar and D. Zazula, "Multichannel blind source separation using convolution kernel compensation," *IEEE Transactions on Signal Processing*, vol. 55, no. 9, pp. 4487–4496, Sep 2007.

[7] ——, "Gradient convolution kernel compensation applied to surface electromyograms," in *International Conference on Independent Component Analysis and Signal Separation*. Springer, Berlin, Heidelberg, 2007, pp. 617–624.

[8] A. Holobar, V. Glaser, J. Gallego, J. L. Dideriksen, and D. Farina, "Non-invasive characterization of motor unit behaviour in pathological tremor," *Journal of Neural Engineering*, vol. 9, no. 5, p. 056011, 2012.

[9] M. Stachaczyk, S. F. Atashzar, S. Dupan, I. Vujaklija, and D. Farina, "Multiclass detection and tracking of transient motor activation based on decomposed myoelectric signals," in *2019 9th International IEEE/EMBS Conference on Neural Engineering (NER)*. IEEE, 2019, pp. 1080–1083.

[10] F. Negro, S. Muceli, A. M. Castronovo, A. Holobar, and D. Farina, "Multi-channel intramuscular and surface EMG decomposition by convolutive blind source separation," *Journal of Neural Engineering*, vol. 13, no. 2, p. 026027, 2016.

[11] J. Thomas, Y. Deville, and S. Hosseini, "Time-domain fast fixed-point algorithms for convolutive ICA," *IEEE Signal Processing Letters*, vol. 13, no. 4, pp. 228–231, 2006.

[12] M. Chen and P. Zhou, "A novel framework based on fastICA for high density surface EMG decomposition," *IEEE Transactions on Neural Systems and Rehabilitation Engineering*, vol. 24, no. 1, pp. 117–127, 2015.

[13] J. Monsifrot, E. Le Carpentier, Y. Aoustin, and D. Farina, "Sequential decoding of intramuscular EMG signals via estimation of a markov model," *IEEE Transactions on Neural Systems and Rehabilitation Engineering*, vol. 22, no. 5, pp. 1030–1040, 2014.

[14] X. Zhu and Y. Zhang, "High-density surface EMG decomposition based on a convolutive blind source separation approach," in *2012 Annual International Conference of the IEEE Engineering in Medicine and Biology Society*. San Diego, CA, USA: IEEE, 2012, pp. 609–612.

[15] H. P. Clamann, "Statistical analysis of motor unit firing patterns in a human skeletal muscle," *Biophysical Journal*, vol. 9, no. 10, pp. 1233–1251, 1969.

[16] R. Person and L. Kudina, "Cross-correlation of electromyograms showing interference patterns," *Electroencephalography and Clinical Neurophysiology*, vol. 25, no. 1, pp. 58–68, Jul 1968.

[17] A. Belouchrani, K. Abed-Meraim, J.-F. Cardoso, and E. Moulines, "A blind source separation technique using second-order statistics," *IEEE Transactions on Signal Processing*, vol. 45, no. 2, pp. 434–444, Feb. 1997.

[18] G. Olmo, F. Laterza, and L. L. Presti, "Matched wavelet approach in stretching analysis of electrically evoked surface EMG signal," *Signal Processing*, vol. 80, no. 4, pp. 671–684, 2000.